Role of the Nuclear Symmetry Energy on the r-mode Instability

Isaac Vidaña
CFisUC, University of Coimbra

CFisUC

Oscillations & Instabilities in Neutron Stars (WG1-WG3 meeting)

September 13th-14th Southampton (UK)

In this talk …

Discuss a couple of aspects of the nuclear symmetry energy that can be relevant for neutron stars.

- ✓ Sensitivity of the core-crust transition to the symmetry energy
- ✓ Role of the symmetry energy on the r-mode instability

For details see:


Phys. Rev. C 83, 045810 (2011)


Phys. Rev. C 85, 045808 (2012)

Neutron-Rich Matter EoS

- <u>Neutron-rich matter</u>

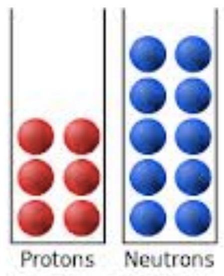

present in:

✓ Nuclei (especially far from stability line)

✓ Astrophysical systems (SN & NS)

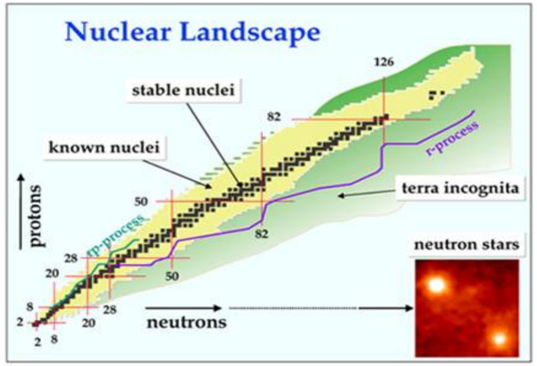

- <u>Charge symmetry</u> ➔ expansion of E/A on even powers of isospin asymmetry $\beta \approx (\rho_n - \rho_p)/(\rho_n + \rho_p)$

$$\frac{E}{A}(\rho,\beta) = E_{SNM}(\rho) + S_2(\rho)\beta^2 + S_4(\rho)\beta^4 + O(6)$$

$$E_{SNM}(\rho) = \frac{E}{A}(\rho,\beta=0), \qquad S_2(\rho) = \frac{1}{2}\left.\frac{\partial^2 E/A}{\partial \beta^2}\right|_{\beta=0}, \qquad S_4(\rho) = \frac{1}{24}\left.\frac{\partial^4 E/A}{\partial \beta^4}\right|_{\beta=0}$$

In good approximation:

$$S_2(\rho) \sim \frac{E}{A}(\rho,\beta=1) - \frac{E}{A}(\rho,\beta=0)$$

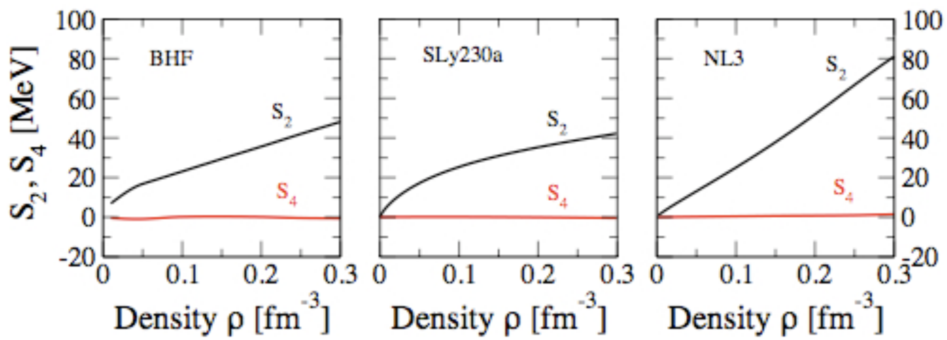

$E_{SNM}(\rho)$ commonly expanded around saturation density ρ_0

$$E_{SNM}(\rho) = E_0 + \frac{K_0}{2}\left(\frac{\rho-\rho_0}{3\rho_0}\right)^2 + \frac{Q_0}{6}\left(\frac{\rho-\rho_0}{3\rho_0}\right)^3 + O(4)$$

$$E_0 = E_{SNM}(\rho=\rho_0) \approx -16\,MeV$$

$$K_0 = 9\rho_0^2 \left.\frac{\partial^2 E_{SNM}(\rho)}{\partial\rho^2}\right|_{\rho=\rho_0} \approx 240 \pm 20\,MeV$$

$$Q_0 = 27\rho_0^3 \left.\frac{\partial^3 E_{SNM}(\rho)}{\partial\rho^3}\right|_{\rho=\rho_0} \approx -500 \div 300\,MeV$$

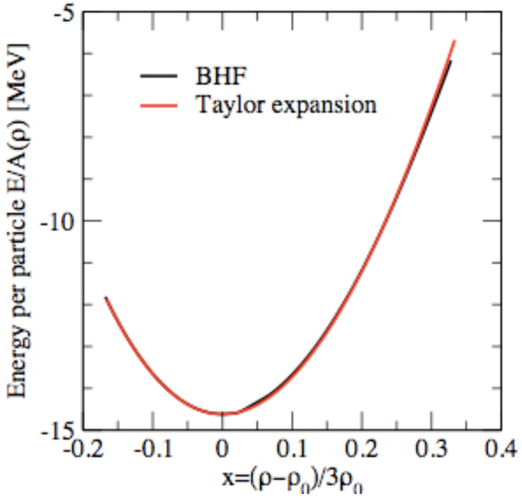

Similarly $S_2(\rho)$ can be also characterized with few bulk parameters around ρ_0

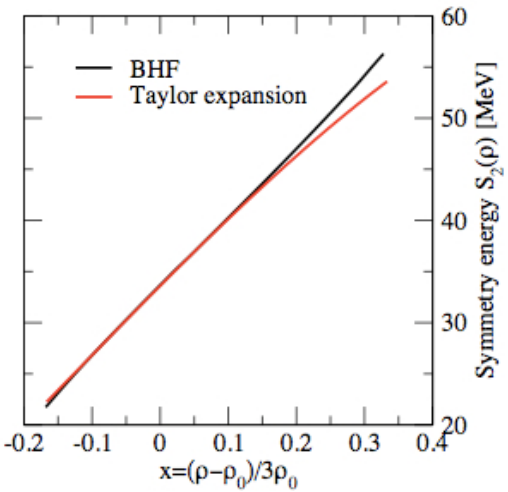

$$S_2(\rho) = E_{sym} + L\left(\frac{\rho-\rho_0}{3\rho_0}\right) + \frac{K_{sym}}{2}\left(\frac{\rho-\rho_0}{3\rho_0}\right)^2 + \frac{Q_{sym}}{6}\left(\frac{\rho-\rho_0}{3\rho_0}\right)^3 + O(4)$$

$$L = 3\rho_0 \left.\frac{\partial S_2(\rho)}{\partial\rho}\right|_{\rho=\rho_0} \quad K_{sym} = 9\rho_0^2 \left.\frac{\partial^2 S_2(\rho)}{\partial\rho^2}\right|_{\rho=\rho_0} \quad Q_{sym} = 27\rho_0^3 \left.\frac{\partial^3 S_2(\rho)}{\partial\rho^3}\right|_{\rho=\rho_0}$$

Less certain & predictions of different models vary largely

Different model predictions

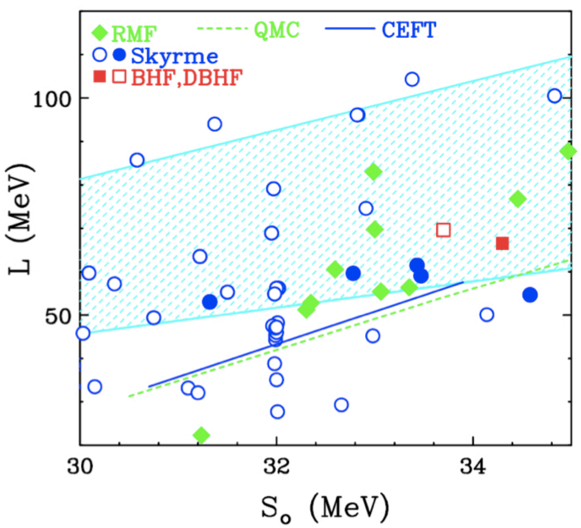

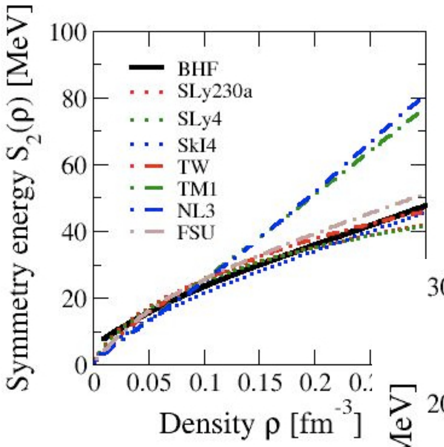

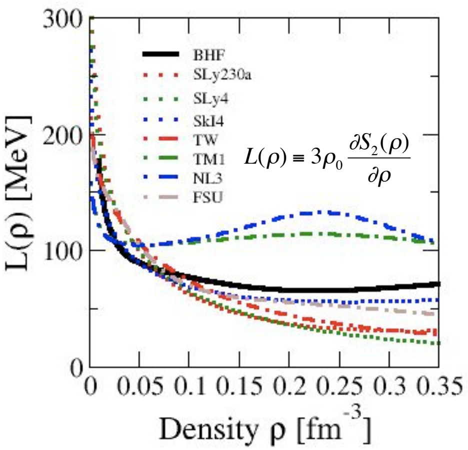

Model	ρ_0 (fm^{-3})	E_0 (MeV)	K_0 (MeV)	Q_0 (MeV)	J (MeV)	L (MeV)	K_{sym} (MeV)	Q_{sym} (MeV)
Microscopic								
BHF-1	0.187	−15.23	195.50	−280.90	34.30	66.55	−31.30	−112.80
Skyrme								
BSk14	0.159	−15.86	239.38	−358.78	30.00	43.91	−152.03	388.30
BSk16	0.159	−16.06	241.73	−363.69	30.00	34.87	−187.39	461.93
BSk17	0.159	−16.06	241.74	−363.73	30.00	36.28	−181.86	450.52
G_σ	0.158	−15.59	237.29	−348.82	31.37	94.02	13.99	−26.77
R_σ	0.158	−15.59	237.41	−348.50	30.58	85.70	−9.13	22.23
LNS	0.175	−15.32	210.83	−382.67	33.43	61.45	−127.37	302.48
NRAPR	0.161	−15.86	225.70	−362.65	32.78	59.63	−123.33	311.63
RATP	0.160	−16.05	239.58	−349.94	29.26	32.39	−191.25	440.74
SV	0.155	−16.05	305.75	−175.86	32.82	96.10	24.19	47.97
SGII	0.158	−15.60	214.70	−381.02	26.83	37.62	−145.92	330.44
SkI2	0.158	−15.78	240.99	−339.81	33.38	104.35	70.71	51.60
SkI3	0.158	−15.99	258.25	−303.96	34.83	100.53	73.07	211.53
SkI4	0.160	−15.95	247.98	−331.26	29.50	60.40	−40.52	351.09
SkI5	0.156	−15.85	255.85	−302.05	36.64	129.34	159.60	11.71
SkI6	0.159	−15.92	248.65	−327.44	30.09	59.70	−47.27	378.96
SkMP	0.157	−15.57	230.93	−338.15	29.89	70.31	−49.82	159.44
SkO	0.160	−15.84	223.39	−392.98	31.97	79.14	−43.17	131.12
Sly230a	0.160	−15.99	229.94	−364.29	31.98	44.31	−98.21	602.92
Sly230b	0.160	−15.98	229.96	−363.21	32.01	45.96	−119.72	521.54
SLy4	0.160	−15.98	229.97	−363.22	32.00	45.94	−119.74	521.58
SLy10	0.156	−15.91	229.74	−358.43	31.98	38.74	−142.19	591.28
Relativistic								
NL3	0.148	−16.24	270.70	188.80	37.34	118.30	100.50	182.60
TM1	0.145	−16.26	280.40	−295.40	36.84	110.60	33.55	−65.20
GM1	0.153	−16.32	299.70	−222.10	32.48	93.87	17.89	25.77
GM3	0.153	−16.32	239.90	−515.50	32.48	89.66	−6.47	55.86
FSU	0.148	−16.30	229.20	−537.40	32.54	60.40	−51.41	426.60
NL$\omega\rho$(025)	0.148	−16.24	270.70	188.80	32.35	61.05	−34.36	1322.00
TW	0.153	−16.25	240.20	−541.00	32.76	55.30	−124.70	539.00
DD-ME1	0.152	−16.23	244.50	307.60	33.06	55.42	−101.00	706.30
DD-ME2	0.152	−16.14	250.90	478.30	32.30	51.24	−87.19	777.10
DDHδI-25	0.153	−16.25	240.20	−540.30	25.62	48.56	81.10	928.30
DDHδII-30	0.153	−16.25	240.20	−540.30	31.89	57.52	80.74	1005.00
NL$\rho\delta$(2.5)	0.160	−16.05	240.40	−470.20	30.71	102.70	127.20	282.90
NL$\rho\delta$(1.7)	0.160	−16.05	240.40	−470.20	30.70	97.14	86.46	202.80
NL$\rho\delta$(0)	0.160	−16.05	240.40	−470.20	30.34	84.51	3.33	61.40

Some properties of asymmetric nuclear matter can be obtained from:

- the analysis of experimental data in heavy ion collisions
  (e.g., ID, double n/p ratios, GDR, …)

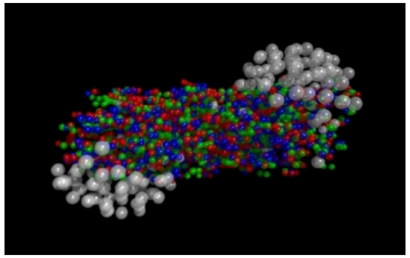

- the analysis of existing correlations between different quantities in bulk matter & finite nuclei
  (e.g. δR versus L)

PREX, CREX experiment @ JLAB

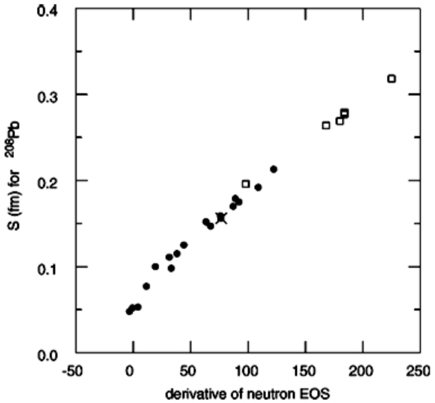

A major effort is being carried out to study experimentally the properties of asymmetric nuclear systems. Experiments at CSR , GSI (FAIR), RIKEN, GANIL, FRIB can probe the behavior of the symmetry energy close and above saturation density.

Astrophysical observations of compact objects
➔ window into nuclear matter at extreme isospin asymmetries

Symmetry Energy Sensitive Observables

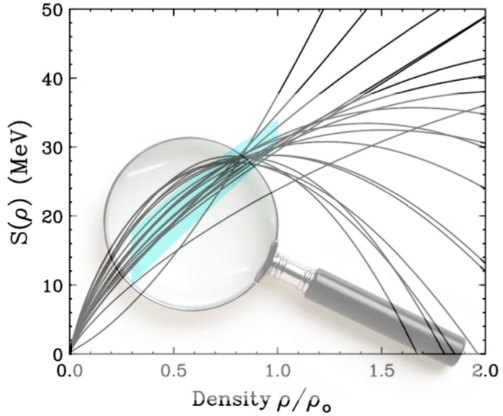

- Sub-saturation densities

✓ Neutron skin thickness in heavy nuclei
✓ Giant & pygmy resonances in neutron-rich nuclei
✓ n/p & t/^{3}He ratios in nuclear reactions
✓ Isospin fragmentation & isospin scaling in nuclear multi-fragmentation
✓ Neutron-proton correlation functions at low relative momenta
✓ Isospin diffusion/transport in heavy ion collisions
✓ Neutron-proton differential flow

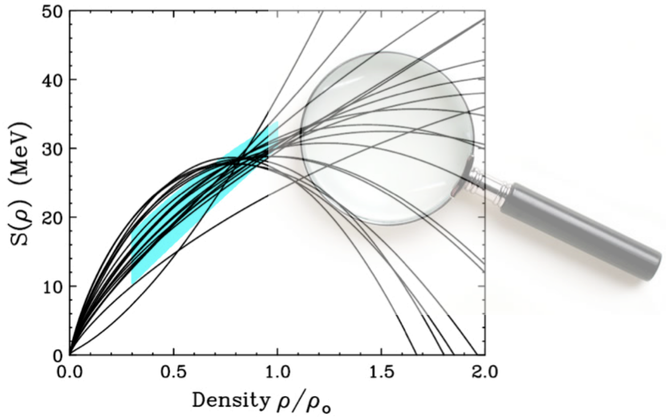

- Supra-saturation densities

✓ π^-/π^+ & K^-/K^+ ratios in heavy ion collisions
✓ Neutron-proton differential transverse flow
✓ n/p ratio of squeezed out nucleons perpendicular to the reaction plane
✓ Nucleon elliptic flow at high transverse momenta

Symmetry Energy & Maximum NS Mass

Larger E_{sym} ➔ Stiffer EoS

➔ Larger NS Mass

Constrain E_{sym} from mass measurements

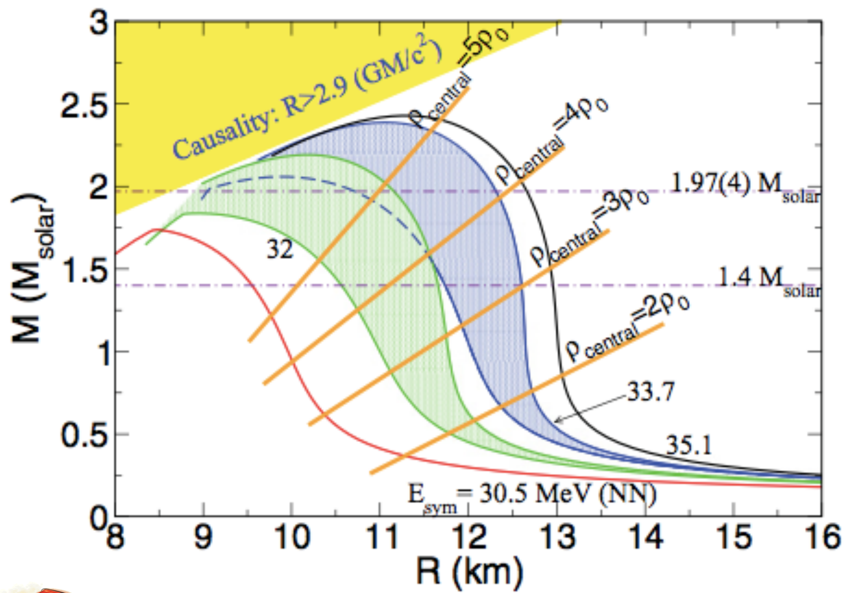

Gandolfi et al., Phys. Rev. C 85, 032801 (R) (2012)

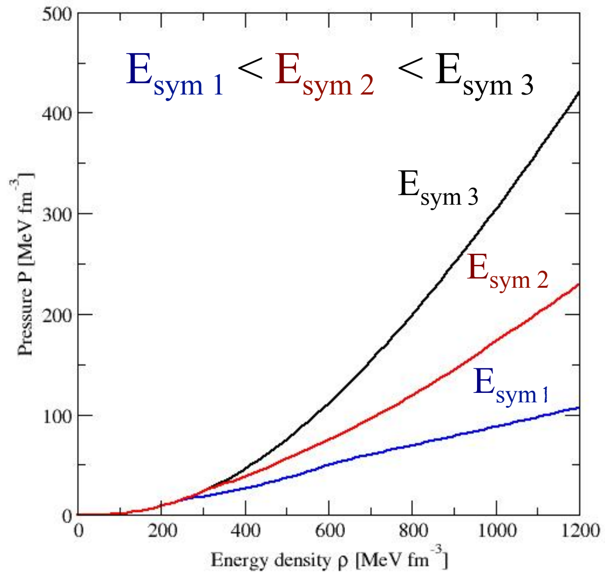

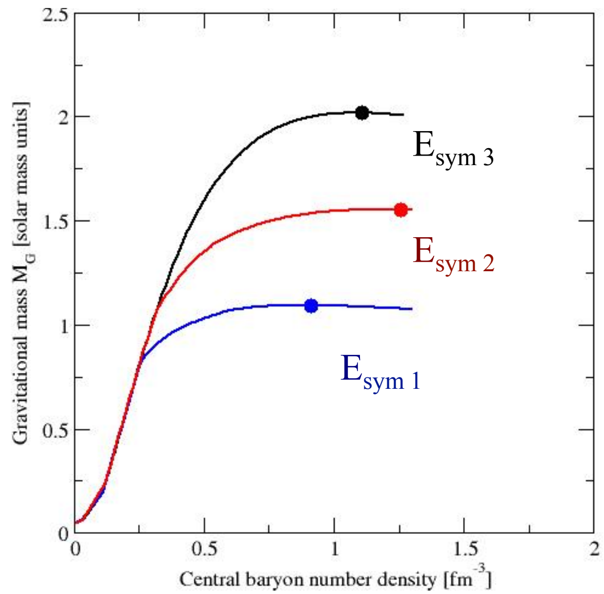

Neutron Star Cooling & Symmetry Energy

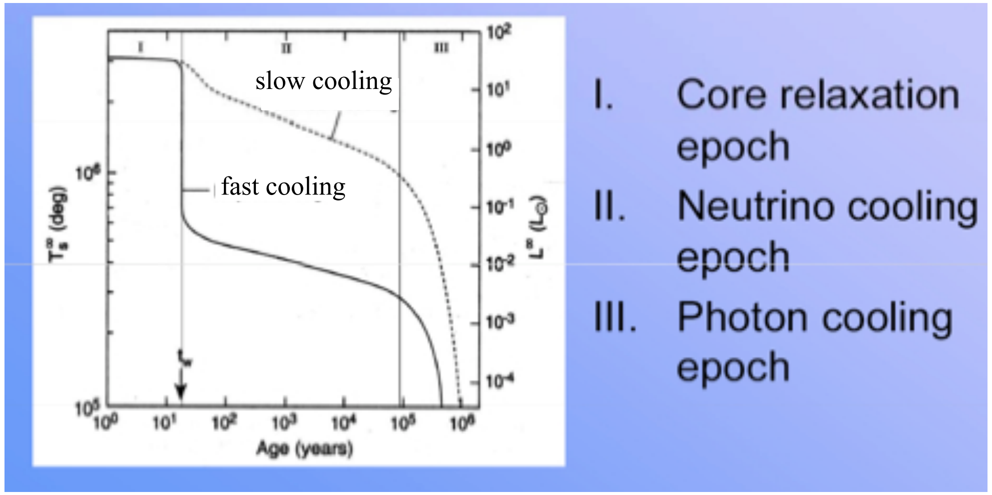

- Fast: e.g., Direct URCA

$$n \rightarrow p + l + \bar{\nu}_l$$
$$l + p \rightarrow n + \nu_l$$

- Slow: e.g., Modified URCA

$$N + n \rightarrow N + p + l + \bar{\nu}_l$$
$$N + l + p \rightarrow N + n + \nu_l$$

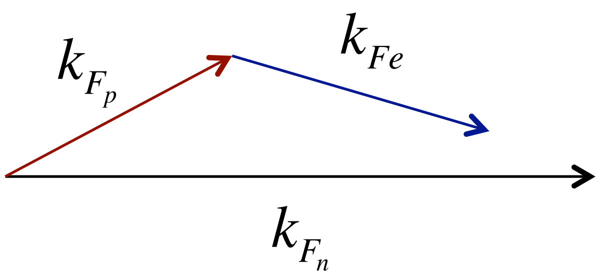

Direct URCA cannot occur unless x_p> 11%-15%

Larger Symmetry Energy ➔ Larger x_p ➔ Earlier onset of Direct URCA

$$\mu_n - \mu_p = 4(1-2x_p)S_2(\rho) = \mu_l - \mu_{\upsilon_l} \Rightarrow \frac{x_p}{1-2x_p} = \frac{4S_2(\rho)}{\hbar c(3\pi^2\rho)^{1/3}}$$

Pressure – Radius Correlation

The analysis of this correlation can put stringent constraints on the symmetry energy

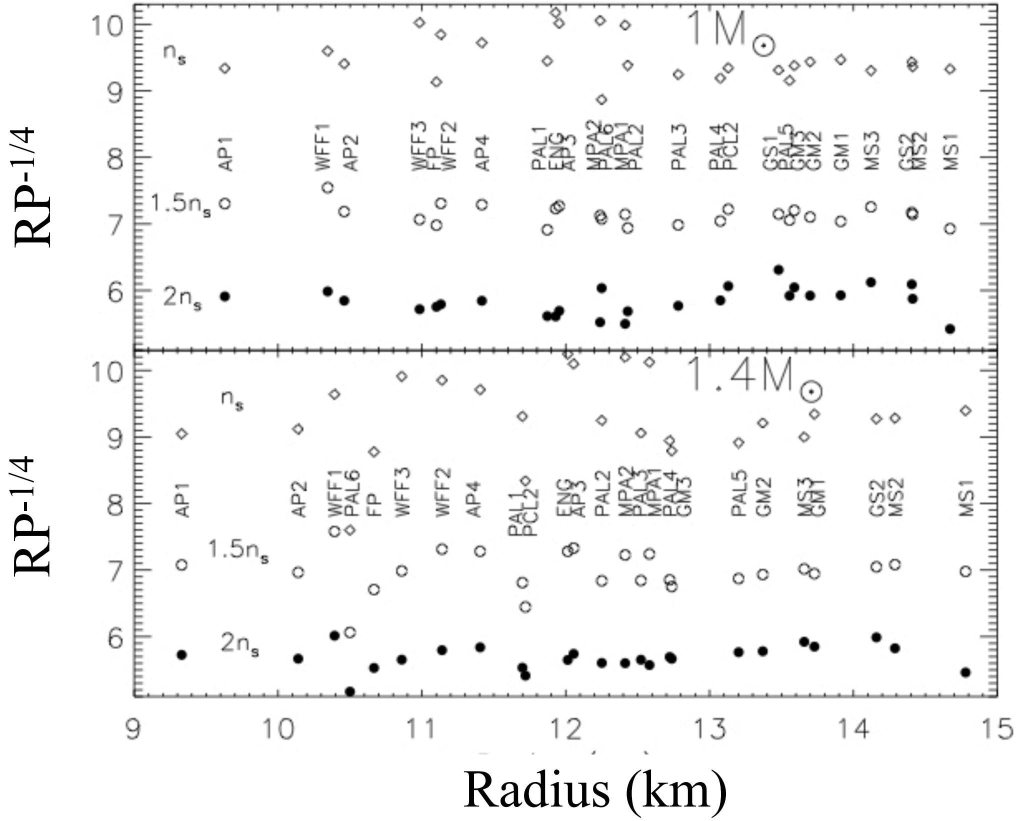

$$P(\rho,\beta) = \frac{\rho^2}{3\rho_0}\left(L\beta^2 + \left(K_0 + K_{sym}\beta^2\right)\frac{\rho-\rho_0}{3\rho_0} + \cdots\right)$$

Lattimer & Prakash, ApJ 550, 426 (2001)

Nevertheless, $E_{sym}(\rho)$ is still uncertain …

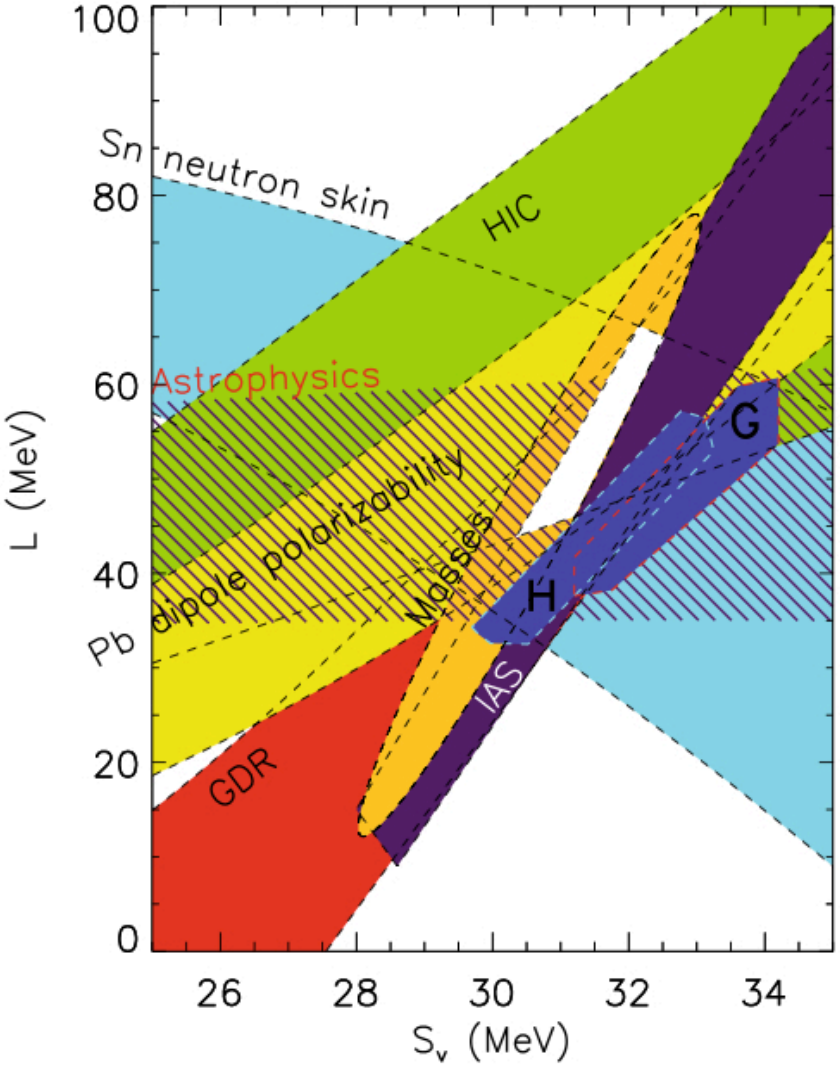

J. M. Lattimer & A. W. Steiner, EPJA 50, 40 (2014)

These two plots summarize our present knowledge or ignorance, if you prefer, on the symmetry energy & its density dependence

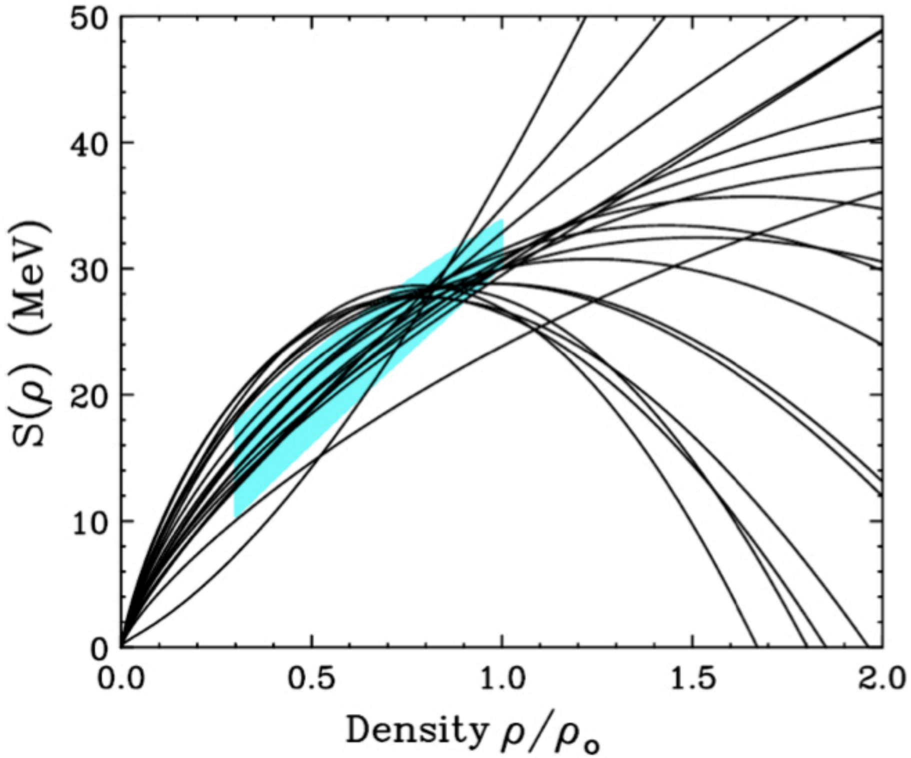

B. A. Brown, PRL 85, 5296 (2001)

Sensitivity of the core-crust transition to the nuclear symmetry energy

Analysis of correlations of L & K_{sym} with crust-core transition point in NS

In collaboration with people you know:

C. Providência

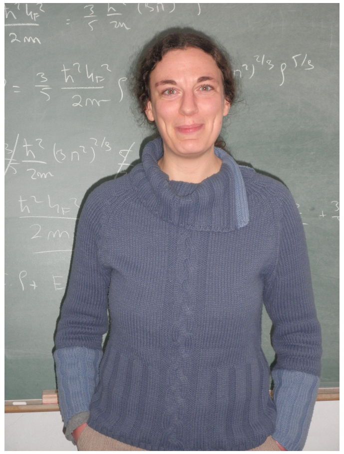

C. Ducoin

J. Margueron

Phys. Rev. C 83, 045810 (2011)

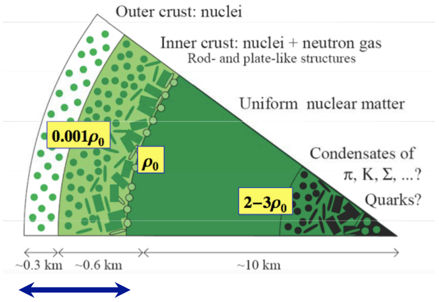

Neutron Stars & Symmetry Energy: Crust-Core transition density

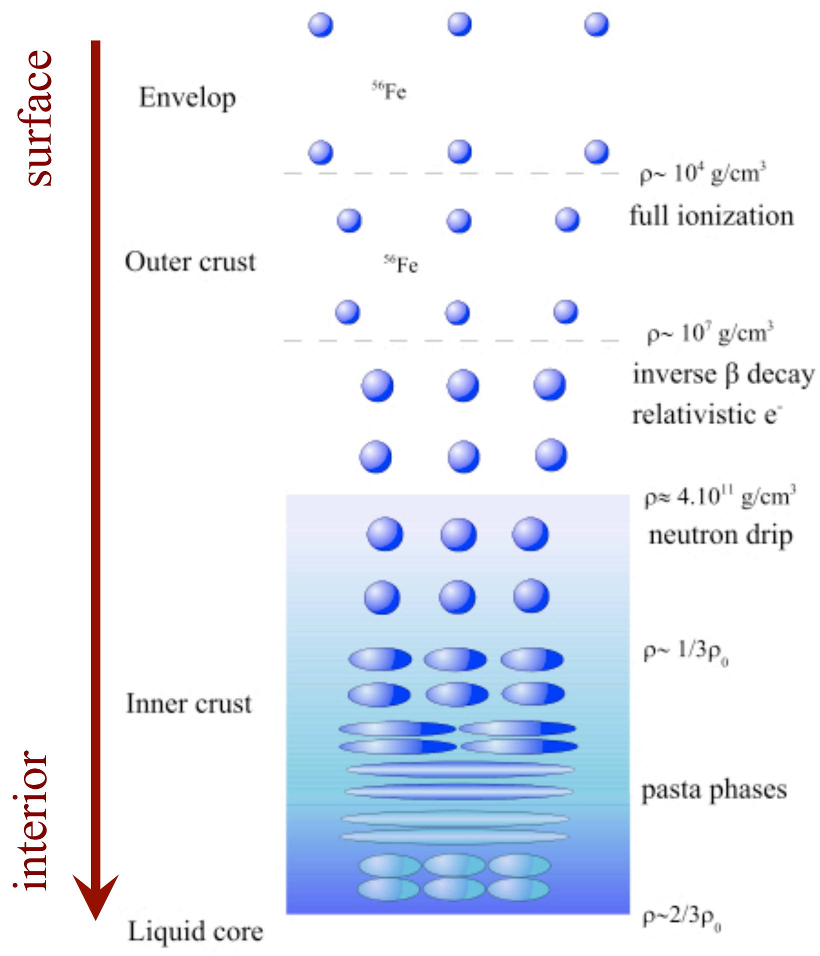

Picture by N. Chamel

The crust of a neutron star is very important for a number of observable properties :

- ✓ thermal evolution
- ✓ glitches
- ✓ X-ray burst
- ….

↓

It is very important to understand well the crust-core transition region

- Which constraints are set by the isospin dependence of the nuclear EoS on the transition region ?
- How sensitive is to the symmetry energy ?

Crust-core transition estimated from crossing of β-equilibrium EoS and spinodal instability line

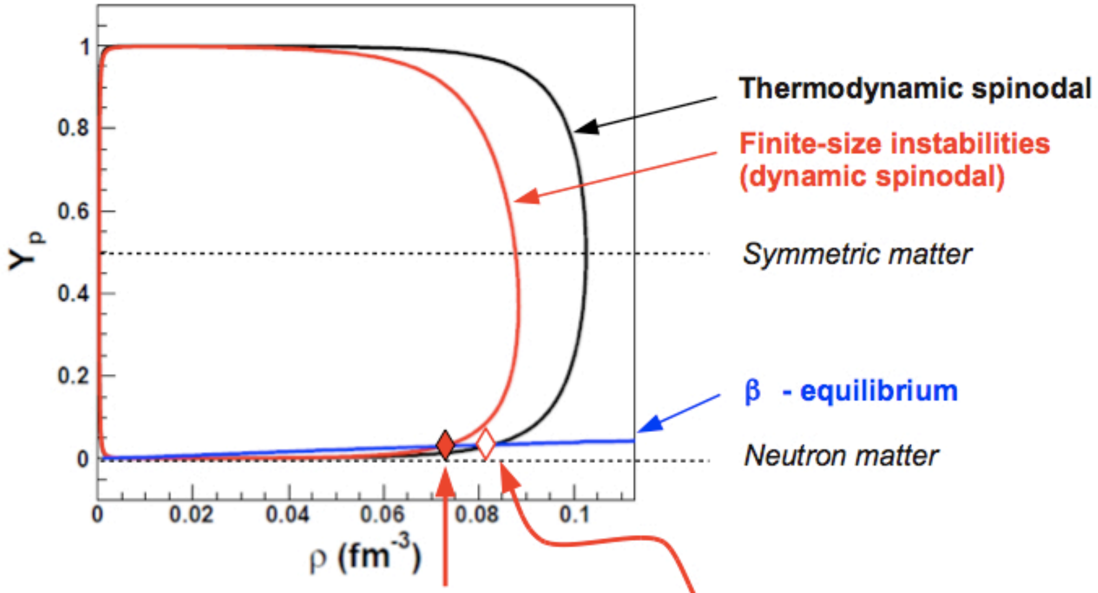

ρ_{td}

ρ_{tt}: we consider first this point

Curvature Matrix:

$$C = \begin{pmatrix} \partial\mu_n/\partial\rho_n & \partial\mu_n/\partial\rho_p & 0 \\ \partial\mu_p/\partial\rho_n & \partial\mu_p/\partial\rho_p & 0 \\ 0 & 0 & \partial\mu_e/\partial\rho_e \end{pmatrix}$$

$$+k^2 \begin{pmatrix} D_{nn} & D_{np} & 0 \\ D_{pn} & D_{pp} & 0 \\ 0 & 0 & 0 \end{pmatrix} + \frac{4\pi e^2}{k_2} \begin{pmatrix} 0 & 0 & 0 \\ 0 & 1 & -1 \\ 0 & -1 & 1 \end{pmatrix}$$

positive definite:

$$Tr(C) > 0, \quad Det(C) > 0$$

Thermodynamical spinodal upper bound of the the real ρ_t (~ 15% larger than TF calculation of nuclear pasta)

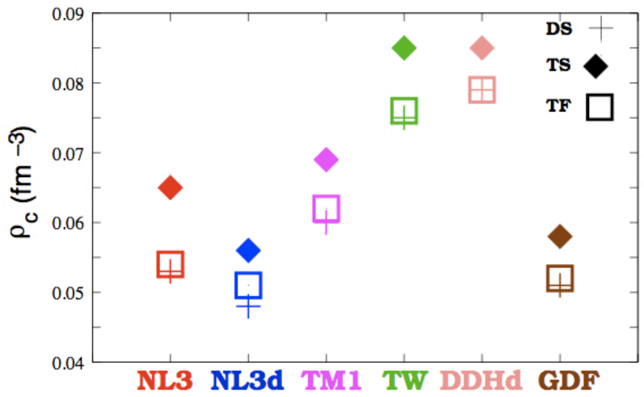

(Figures courtesy of C. Ducoin & C.Providência)

Microscopic approaches

✧ BHF with Av18 + UIX

- $$\frac{E}{A}(\rho,\beta)=\frac{1}{A}\sum_{\tau}\sum_{k\le k_{F_\tau}}\left(\frac{\hbar^2k^2}{2m_\tau}+\frac{1}{2}\mathrm{Re}\left[U_\tau(\vec{k})\right]\right)$$

Infinite sumation of two-hole line diagrams

✓ $$G(\omega)=V+V\frac{Q}{\omega-E-E^{'}+i\eta}G(\omega)$$

✓ $$E_\tau(k)=\frac{\hbar^2k^2}{2m_\tau}+\mathrm{Re}\left[U_\tau(k)\right]$$

✓ $$U_\tau(k)=\sum_{\tau'}\sum_{k'\le k_{F_{\tau'}}}\left\langle \vec{k}\vec{k}'\middle|G(\omega=E_\tau(k)+E_{\tau'}(k'))\middle|\vec{k}\vec{k}'\right\rangle_{\mathcal{A}}$$

Partial sumation of pp ladder diagrams

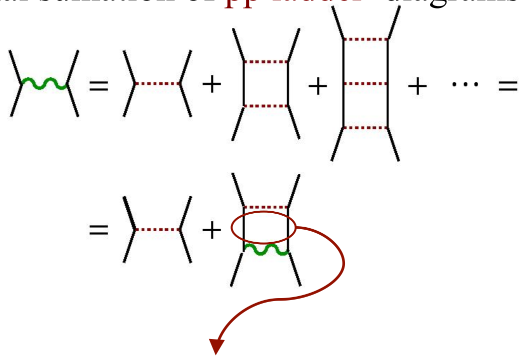

✓ Pauli blocking
✓ Nucleon dressing

✧ APR & AFDMC parametrized

- $$\frac{E}{A}(\rho,\beta)=E_0u\frac{u-2-s}{1+us}+S_0u^\gamma\beta^2, \qquad u=\rho/\rho_0$$ Heiselberg & Hjorth-Jensen Phys. Rep. 328, 237 (2000)

- $$\frac{E}{A}(\rho,\beta)=E_0+a(\rho-\rho_0)^2+b(\rho-\rho_0)^3e^{\gamma(\rho-\rho_0)}+C_s\left(\frac{\rho}{\rho_0}\right)^{\gamma_s}\beta^2$$ Gandolfi et al., MNRAS 404, L35 (2010)

Phenomenological approaches

✧ Skyrme

- Lyon group SLy: SLy0-SLy10, Sly230a
- SkI family: SkI1-SkI6
- Rs, Gs, SGI, SkMP, SkO, SkO', SkT4-5, SV

✧ Relativistic mean field models

- Non-linear Walecka models (NLWM) with constant coupling constants: GM1, GM3, TM1, NL3, NL3-II, NL-SH

- Density dependent hadronic models (DDH) with density dependent coupling constants: DDME1, DDME2, TW99, PK1, PK1R, PKDD

Correlation of Y_{pt} and ρ_t with L

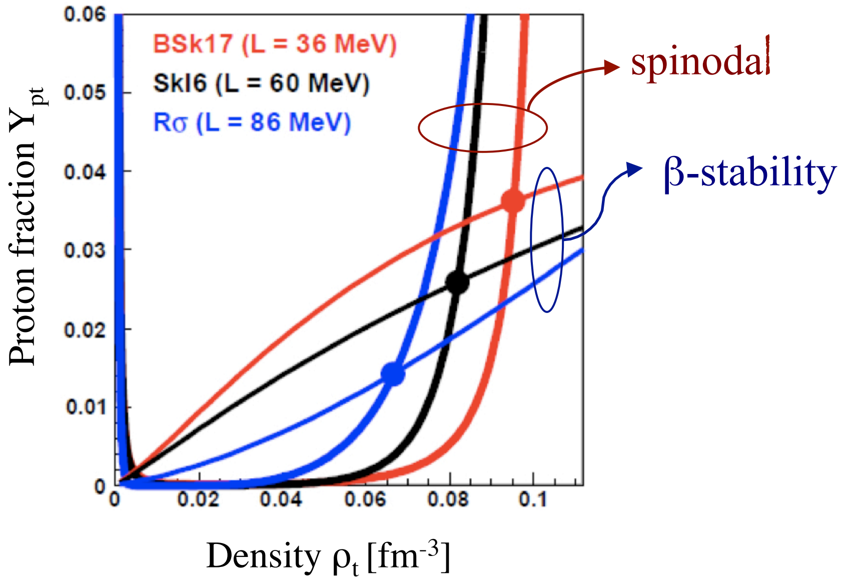

✓ Clear decreasing correlations

Higher L ➔ { Lower Y_{pt}, Lower ρ_t }

✓ Dispersion of Y_{pt} due to dispersion of E_{sym}

$$\left(\mu_n - \mu_p = 4\beta S_2(\rho) = \mu_e - \mu_{\nu_e} \Rightarrow \frac{Y_p^{1/3}}{(1-2Y_p)} = \frac{4S_2(\rho)}{\hbar c\left(3\pi^2\rho\right)^{1/3}} \right)$$

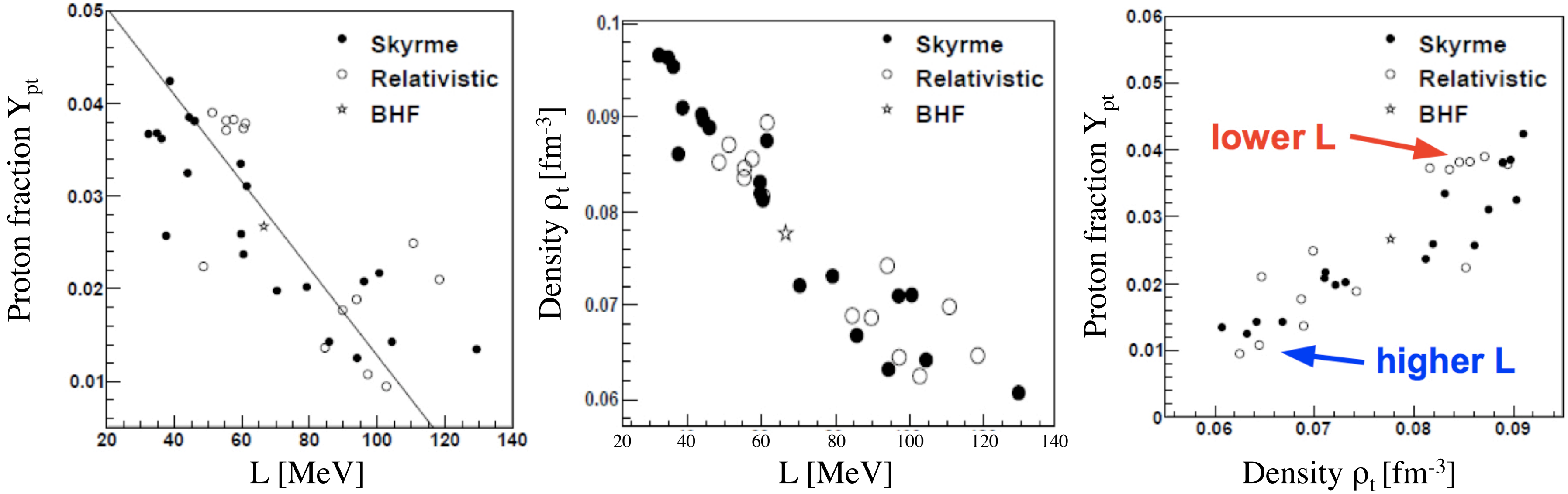

L- P_t correlation: an open issue

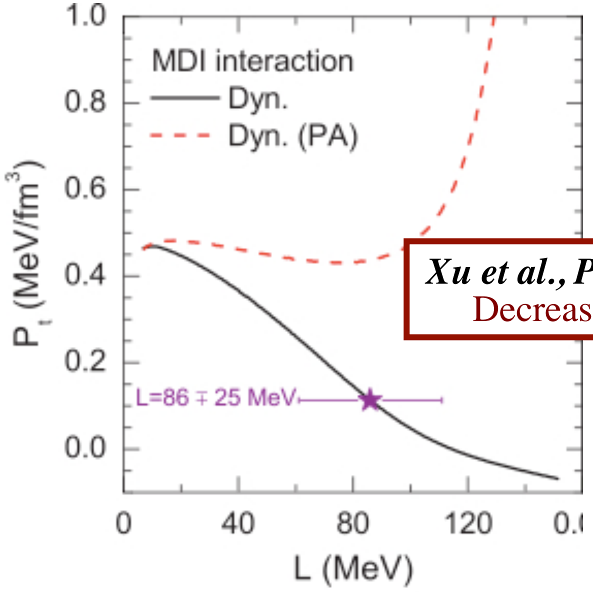

Xu et al., PRC, 2009
Decrease of P_t

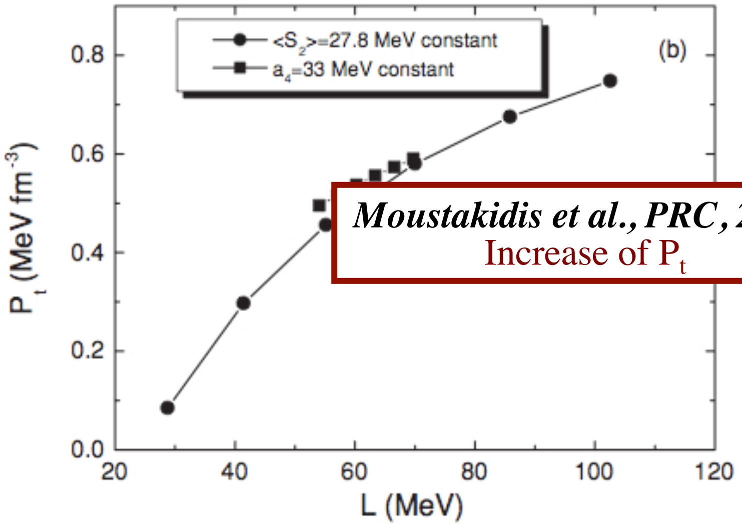

Moustakidis et al., PRC, 2010
Increase of P_t

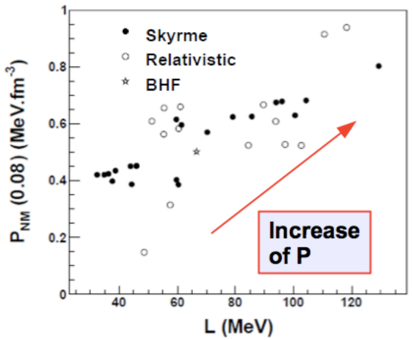

Increase of P with L in n-rich matter at fixed density

$$P(\rho,\beta)=\frac{\rho^2}{3\rho_0}\left(L\beta^2+\left(K_0+K_{sym}\beta^2\right)\frac{\rho-\rho_0}{3\rho_0}+\cdots\right)$$

BUT P_t shows dispersion

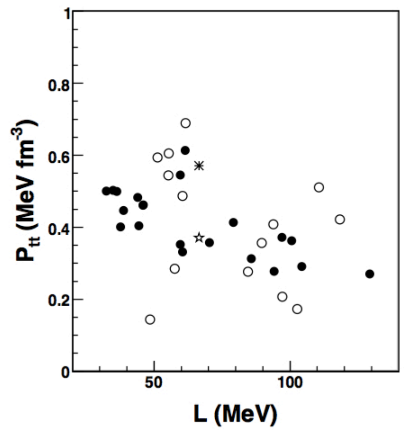

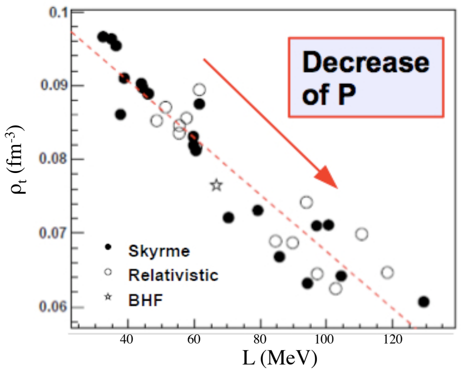

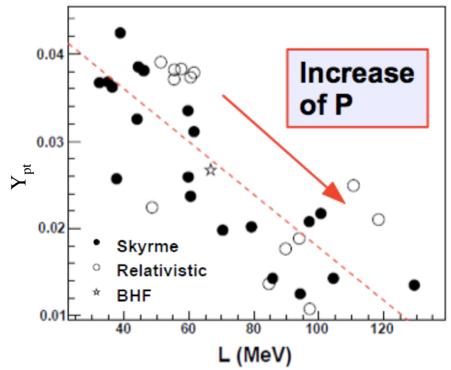

Role of other bulk parameters

Dynamical vs Themodynamical spinodal

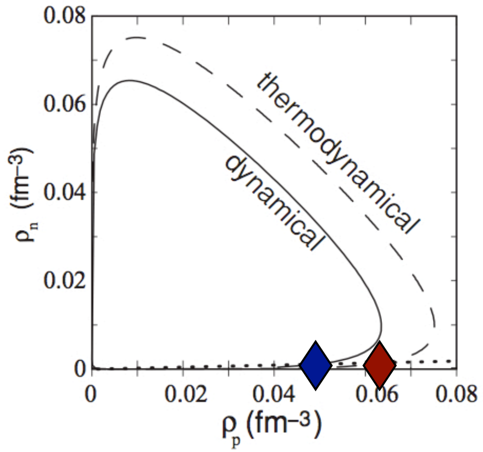

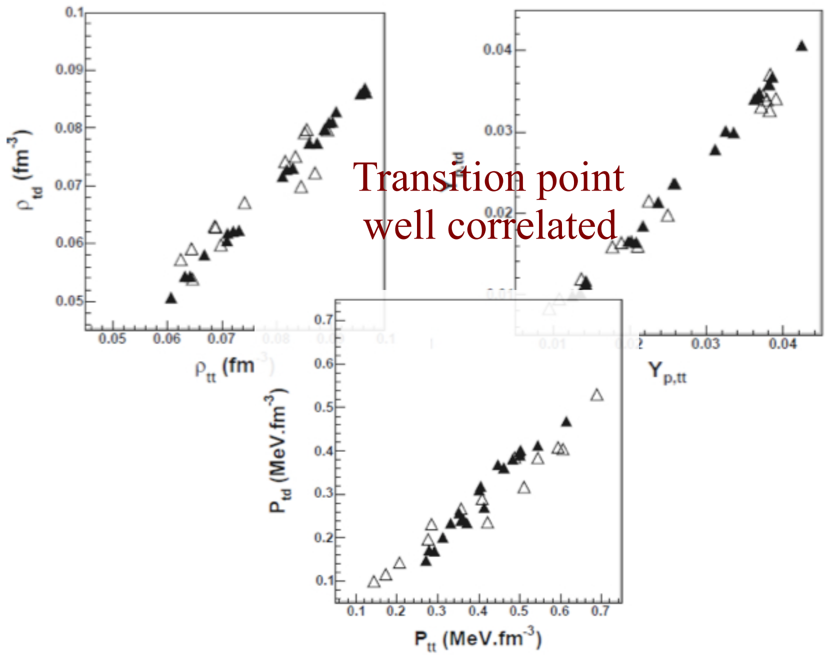

Transition point
well correlated

Fits on pairs of parameters

$$P_t = aX_1 + bX_2 + c$$

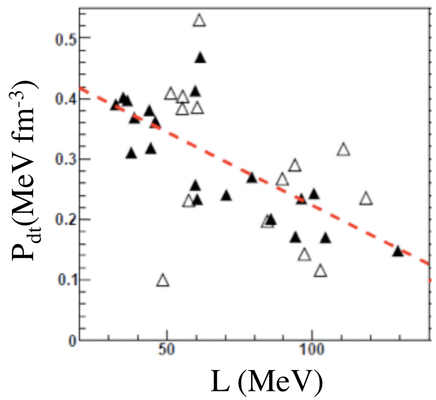

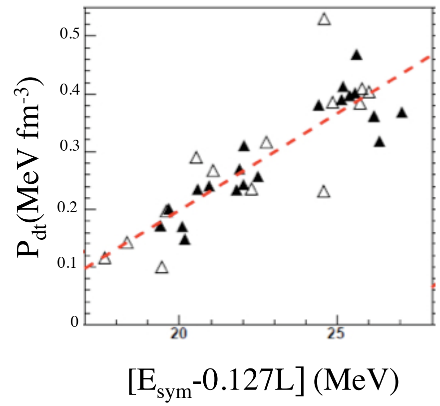

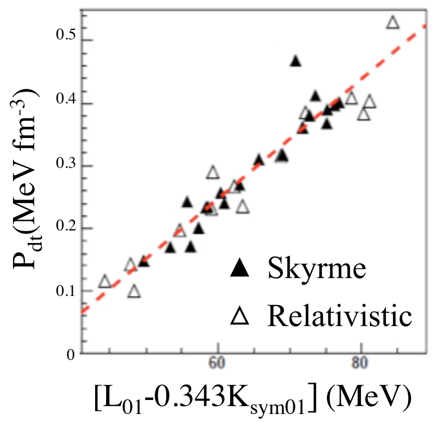

- ✓ Unclear L-P_t correlation
- ✓ Inclusion of E_{sym} ➔ more reliable corelation
- ✓ Good correlation with L and K_{sym} at ρ=0.1 fm^{-3}

Correlation of the Neutron Skin Thickness δR with L & K_{sym}

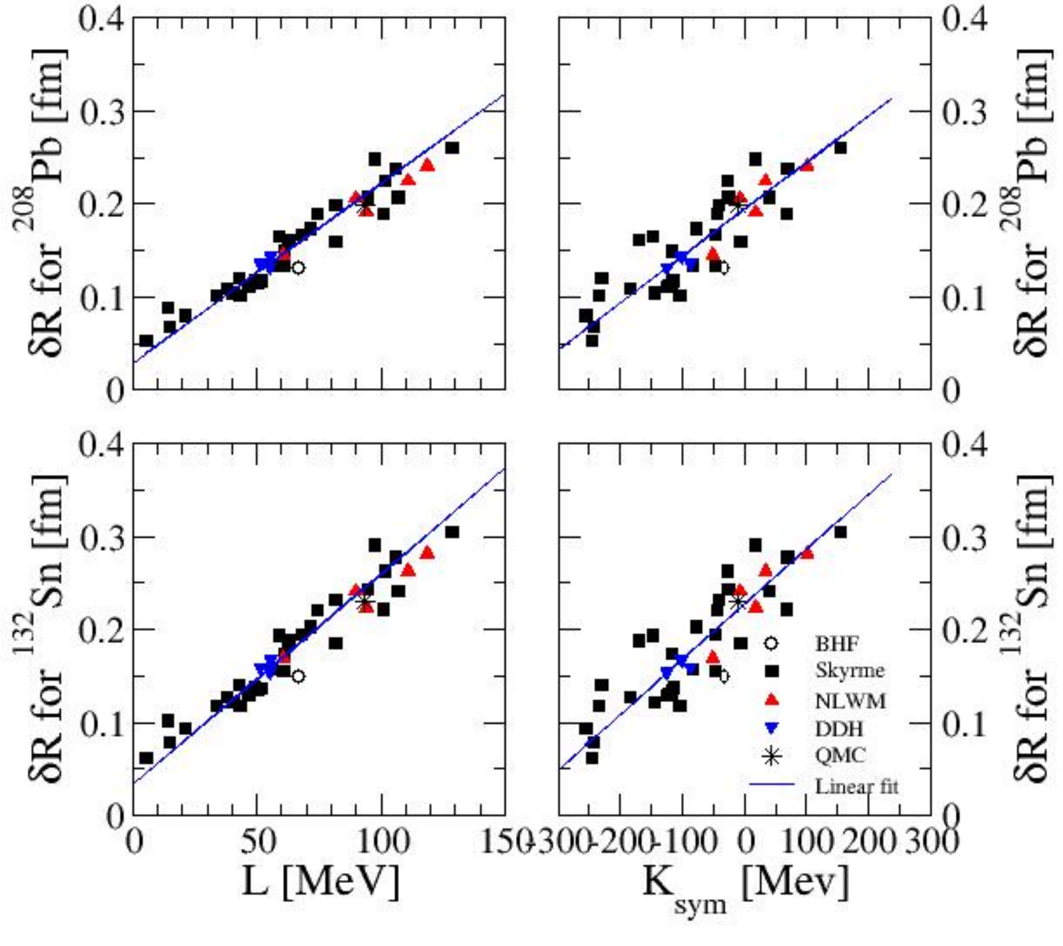

Linear increase of δR with L & K_{sym}

Not surprising:

- ✓ Pressure ➔ δR
- ✓ In n-rich matter pressure increases with L at fixed ρ

$$P(\rho,\beta)=\frac{\rho^2}{3\rho_0}\left(L\beta^2+\left(K_0+K_{sym}\beta^2\right)\frac{\rho-\rho_0}{3\rho_0}+\cdots\right)$$

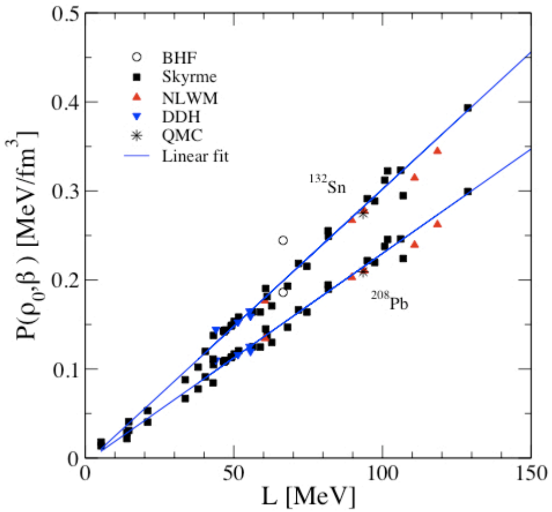

Phys. Rev. C 80, 045806 (2009)

Neutron Skin Thickness & The Crust-Core Transition Density

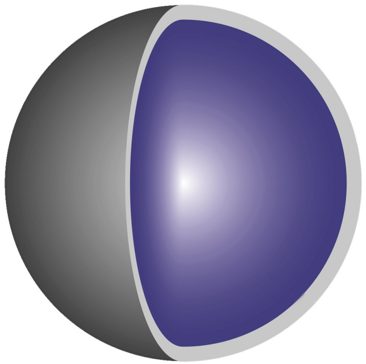

Neutron Star

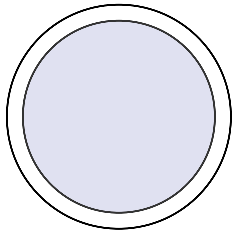

Heavy nucleus

Neutron Star Crust & Neutron Skin are made out of neutron rich matter at similar densities

↓

Both are governed by EoS at subnuclear densities in particular by $S_2(\rho)$ & its derivatives

Inverse correlation between δR and ρ_t (Horowiz & Piekarewicz)

↓

an accurate measurement of neutron skin in neutron rich nuclei can provide considerable & valuable information on the crust-core transition density.

(PREX, CREX experiment @ JLAB)

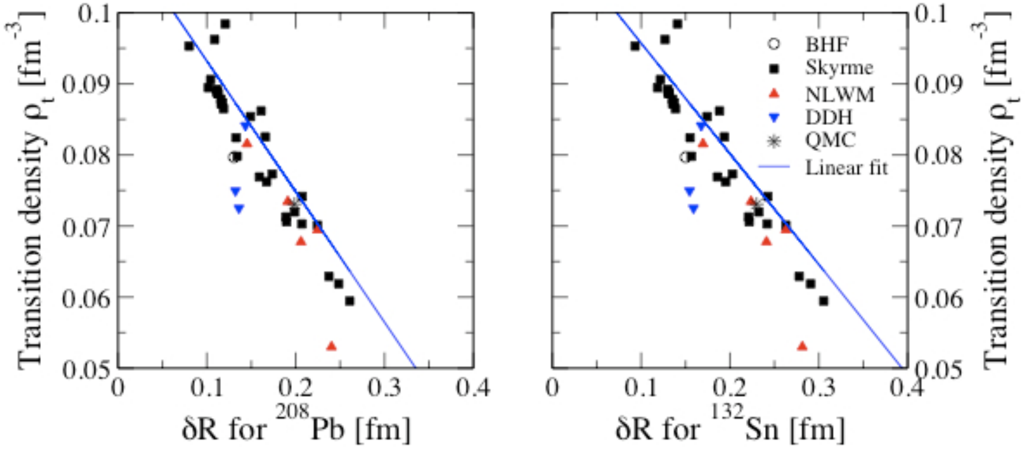

Role of the symmetry energy on the r-mode instability

Study the role of the symmetry energy slope parameter L on the r-mode instability of neutron stars by using both microscopic (BHF, APR & AFDMC) and phenomenological (Skyrme & RMF) approaches of the nuclear matter EoS

Phys. Rev. C 85, 045808 (2012)

The r-mode instability in a nutshell
(sure you know better than me)

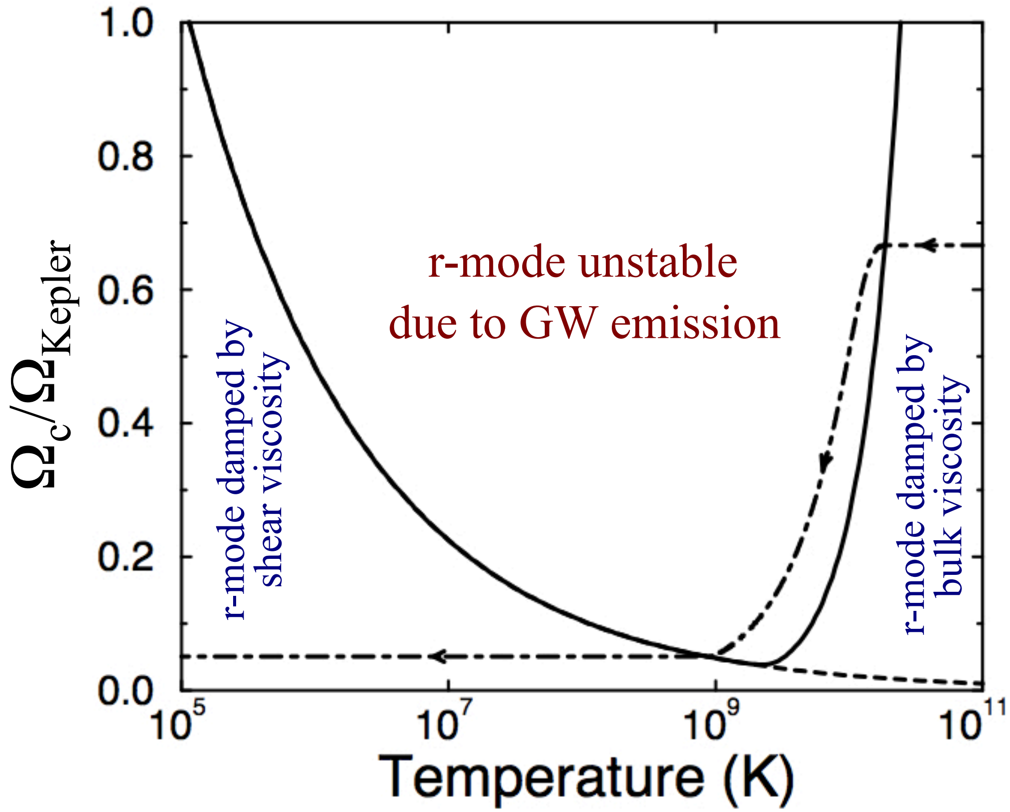

r-mode instability : toroidal mode of oscillation

✓ restoring force: Coriolis

✓ emission of GW (CFS mechanism)

- GW makes the mode unstable
- Viscosity stabilizes the mode

$$A \propto A_0 e^{-i\omega(\Omega) - t/\tau(\Omega,T)}$$

$$\frac{1}{\tau(\Omega,T)} = -\frac{1}{\tau_{GW}(\Omega)} + \frac{1}{\tau_{Viscosity}(\Omega,T)}$$

N. Andersson, Astrophys. J 502, 708 (1998)

J. L. Friedman & S. M. Morsink , Astrophys. J 502, 714 (1998)

Bulk & shear viscosities

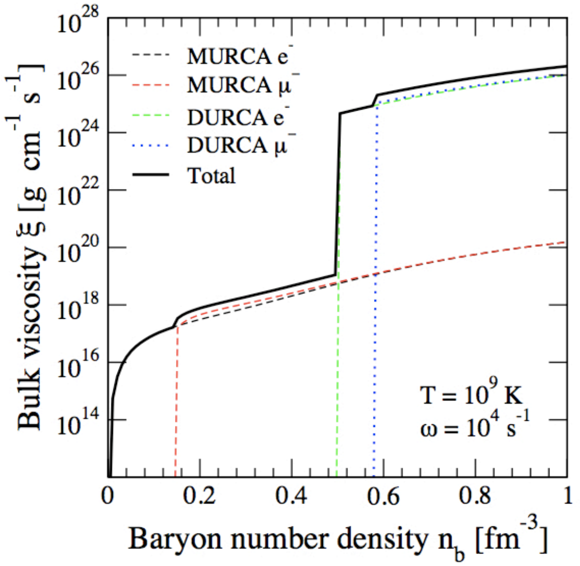

✓ Modified URCA

$$\zeta_{ne0} = \frac{367\, G_F^2\, g_A^2\, m_n^{*3}\, m_p^*\, p_{Fp}\, C_e^2}{1512\,\pi^3\,\hbar^{10}\,c^8\,\omega^2}\left(\frac{f^\pi}{m_\pi}\right)^4 (k_B T)^6\,\alpha,$$
$$\approx 1.49\;10^{19}\left(\frac{m_n^*}{m_n}\right)^3\frac{m_p^*}{m_p}\left(\frac{n_p}{n_0}\right)^{1/3}\left(\frac{C_e}{100\,\mathrm{MeV}}\right)$$
$$\times T_9^6\,\omega_4^{-2}\,\alpha_n\,\beta_n \quad \mathrm{g\ cm^{-1}s^{-1}},$$
$$\zeta_{pe0} = \zeta_{ne0}\left(\frac{m_p^*}{m_n^*}\right)^2\frac{(3\,p_{Fp}+p_{Fe}-p_{Fn})^2}{8\,p_{Fp}\,p_{Fe}}\,\Theta_{pe},$$

$$\zeta_{n\mu 0} = \zeta_{ne0}\left(\frac{p_{F\mu}}{p_{Fe}}\right)\left(\frac{C_\mu}{C_e}\right)^2,$$
$$\zeta_{p\mu 0} = \zeta_{ne0}\left(\frac{C_\mu m_p^*}{C_e m_n^*}\right)^2\frac{(3p_{Fp}+p_{F\mu}-p_{Fn})^2}{8\,p_{Fp}\,p_{F\mu}}\left(\frac{p_{F\mu}}{p_{Fe}}\right)\Theta_{p\mu},$$

✓ Direct URCA

$$\zeta_{l0} = \frac{17\,G^2(1+3g_A^2)C_l^2}{240\pi\hbar^{10}c^3\,\omega^2}\,m_n^* m_p^* m_e^*\,(k_B T)^4\;\Theta_{npl}$$
$$= 8.553\times 10^{24}\,\frac{m_n^*}{m_n}\,\frac{m_p^*}{m_p}\left(\frac{n_e}{n_0}\right)^{1/3}$$
$$\times T_9^4\,\frac{1}{\omega_4^2}\left(\frac{C_l}{100\,\mathrm{MeV}}\right)^2\Theta_{npl}\;\mathrm{g\,cm^{-1}\,s^{-1}},$$

Haensel et al., AA 357, 1157 (2000); AA 372, 130 (2001)

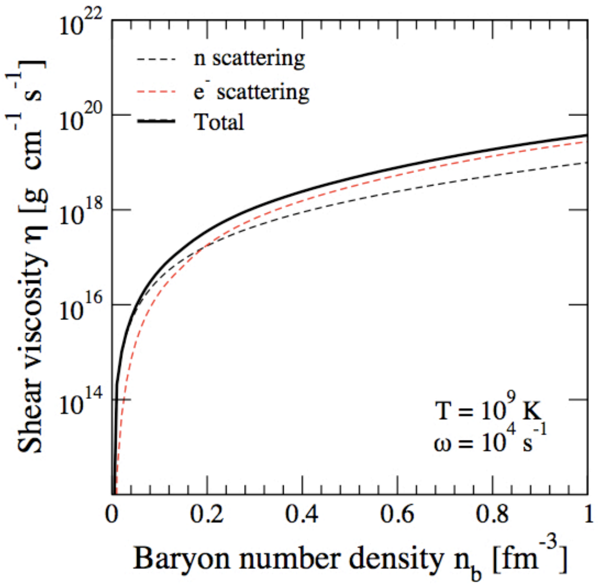

$$\eta = \eta_n + \eta_e$$

✓ n scattering [1]

$$\eta_n = 2\times 10^{18}\left(\frac{\rho}{10^{15}\,gcm^{-3}}\right)^{9/4}\left(\frac{T}{10^9 K}\right)^{-2}$$

✓ e⁻ scattering [2]

$$\eta_e = 4.26\times 10^{-26}\left(x_p n_b\right)^{14/9} T^{-5/3}$$

[1] Cutler & Lindblom., ApJ 314, 234 (1987)
[2] Shternin & Yakovlev, PRD 78, 063006 (2008)

L dependence of ξ and η

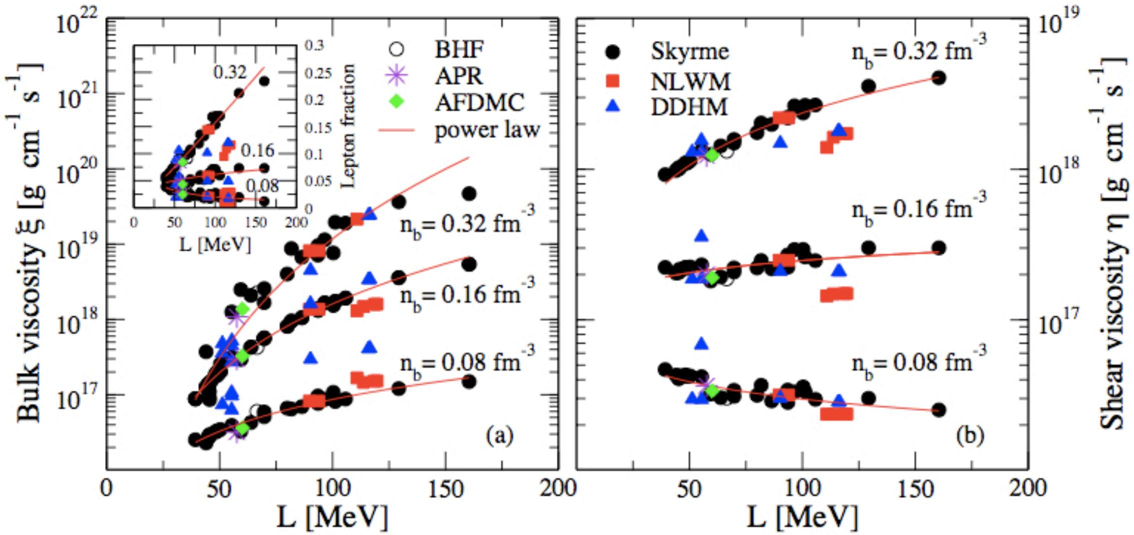

✓ ξ increases with L for all densities

✓ η increases with L for $n_b > n_0$ & decreases with L for $n_b < n_0$

consequence of lepton fraction dependence

L dependence described by simple power laws

$$\xi = A_\xi L^{B_\xi}, \eta = A_\eta L^{B_\eta}$$

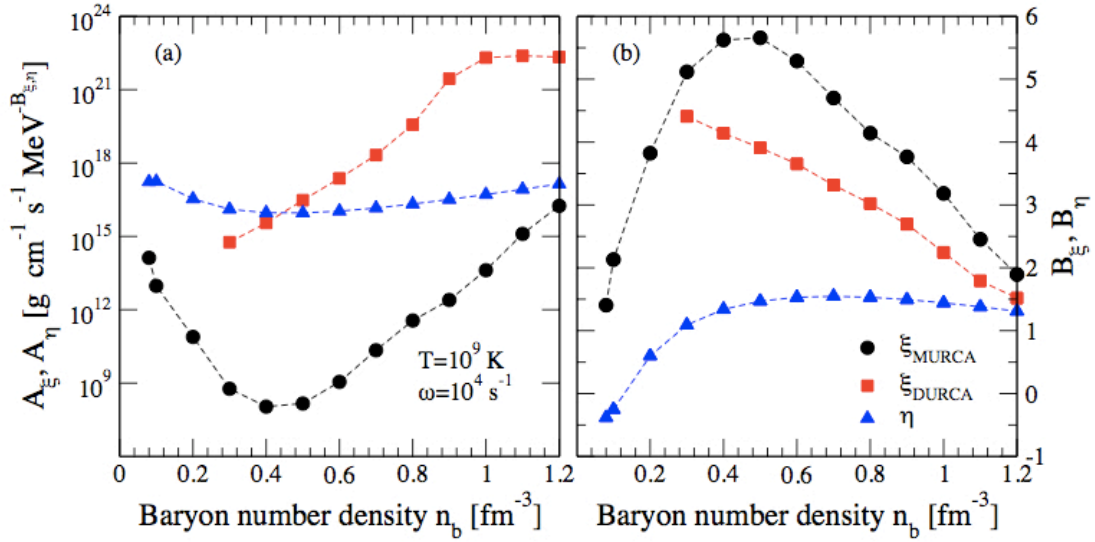

Dissipative time scales of r-modes

$$\frac{1}{\tau_i} = -\frac{1}{2E}\left(\frac{dE}{dt}\right)_i$$

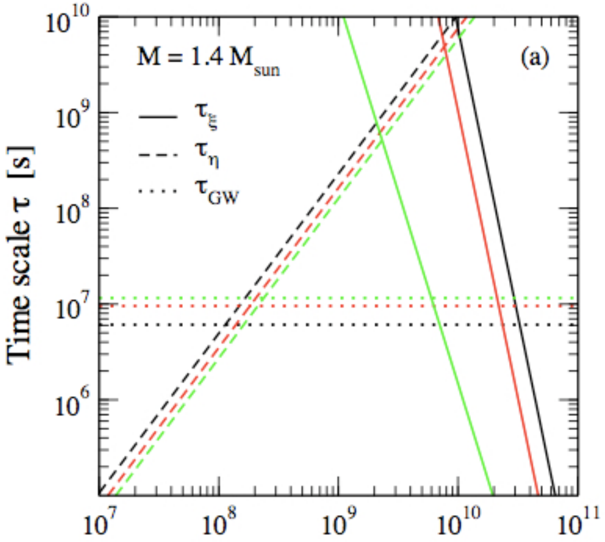

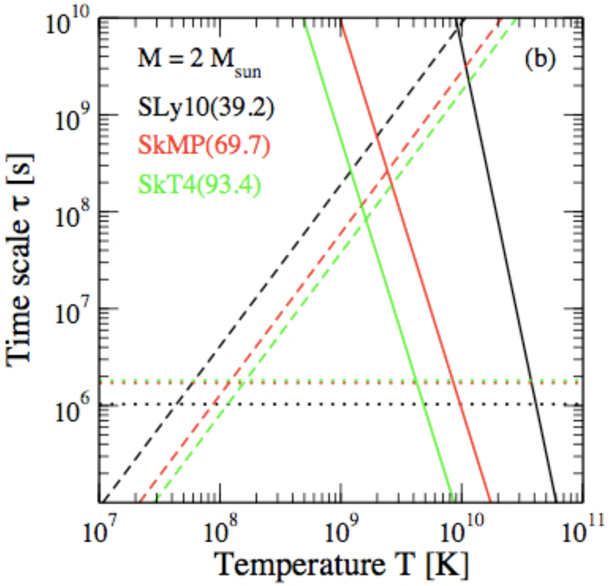

- $$\frac{1}{\tau_\xi} = \frac{4\pi}{690}\left(\frac{\Omega^2}{\pi G\bar{\rho}}\right)^2 R^{2l-2}\left[\int_0^R \rho r^{2l+2} dr\right]^{-1}\int_0^R \xi\left(\frac{r}{R}\right)^2\left[1+0.86\left(\frac{r}{R}\right)^2\right] r^2 dr$$
- $$\frac{1}{\tau_\eta} = (l-1)(2l+1)\left[\int_0^R \rho r^{2l+2} dr\right]^{-1}\int_0^R \eta r^{2l} dr$$
- $$\frac{1}{\tau_{GW}} = \frac{32\pi G\Omega^{2l+2}}{c^{2l+3}}\frac{(l-1)^{2l}}{[(2l+1)!!]^2}\left(\frac{l+2}{l+1}\right)^{2l+1}\int_0^R \rho r^{2l+2} dr$$

✓ τ_{GW} larger for models with larger L

Larger L ➔ stiffer EoS ➔ less compact star ➔ τ_{GW} larger

✓ τ_ξ & τ_η smaller for models with larger L

τ_ξ (τ_η) decrease with $\xi(\eta)$ but $\xi(\eta)$ increase with L

✓ τ_{GW}, τ_ξ & τ_η decrease when increasing M

Given an EoS: the more massive the star the denser it is

➔ τ_{GW}, $\tau_\xi \sim (\rho/\xi)R^2$ & $\tau_\eta \sim (\rho/\eta)R^2$ decrease

R-mode instability region

- time dependence of an r-mode $\sim e^{i\omega t - t/\tau}$

$$\frac{1}{\tau(\Omega,T)} = -\frac{1}{\tau_{GW}(\Omega)} + \frac{1}{\tau_{\xi}(\Omega,T)} + \frac{1}{\tau_{\eta}(T)}$$

➔ $\frac{1}{\tau(\Omega_c,T)} = 0$ r-mode instability region

$\Omega < \Omega_c$ stable

$\Omega > \Omega_c$ unstable

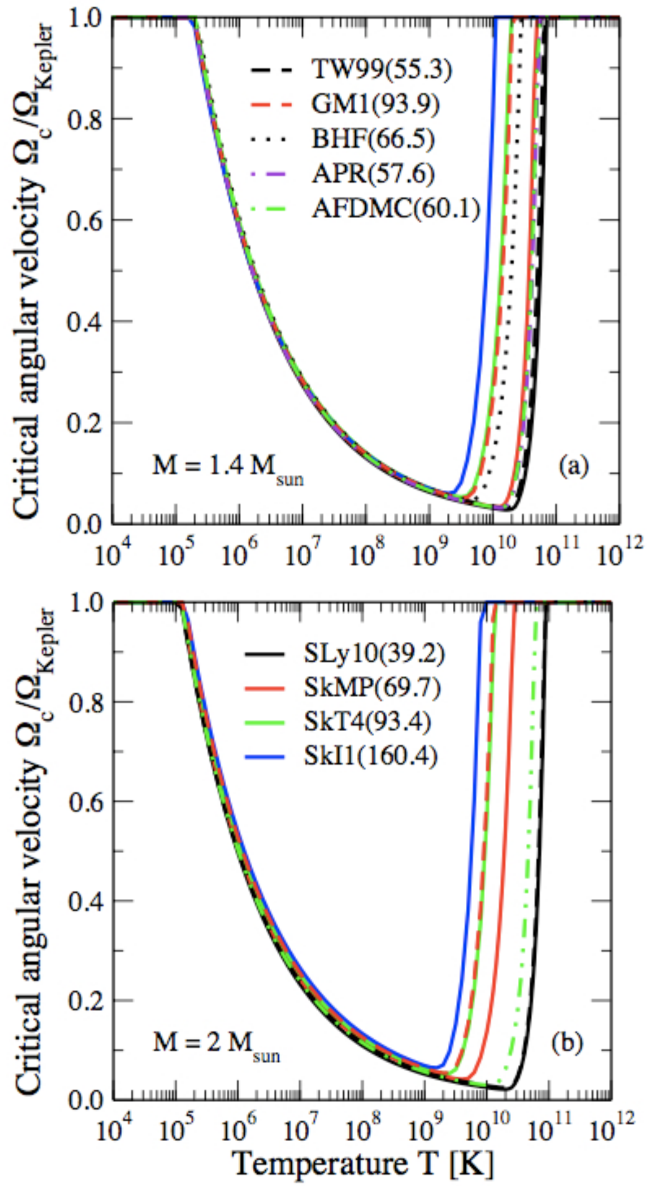

✓ instability region smaller for models with larger L (increase of ξ & η with L)

✓ instability region larger for more massive star (time scales decrease when M increases)

Is it possible to constrain L from LMXB ?

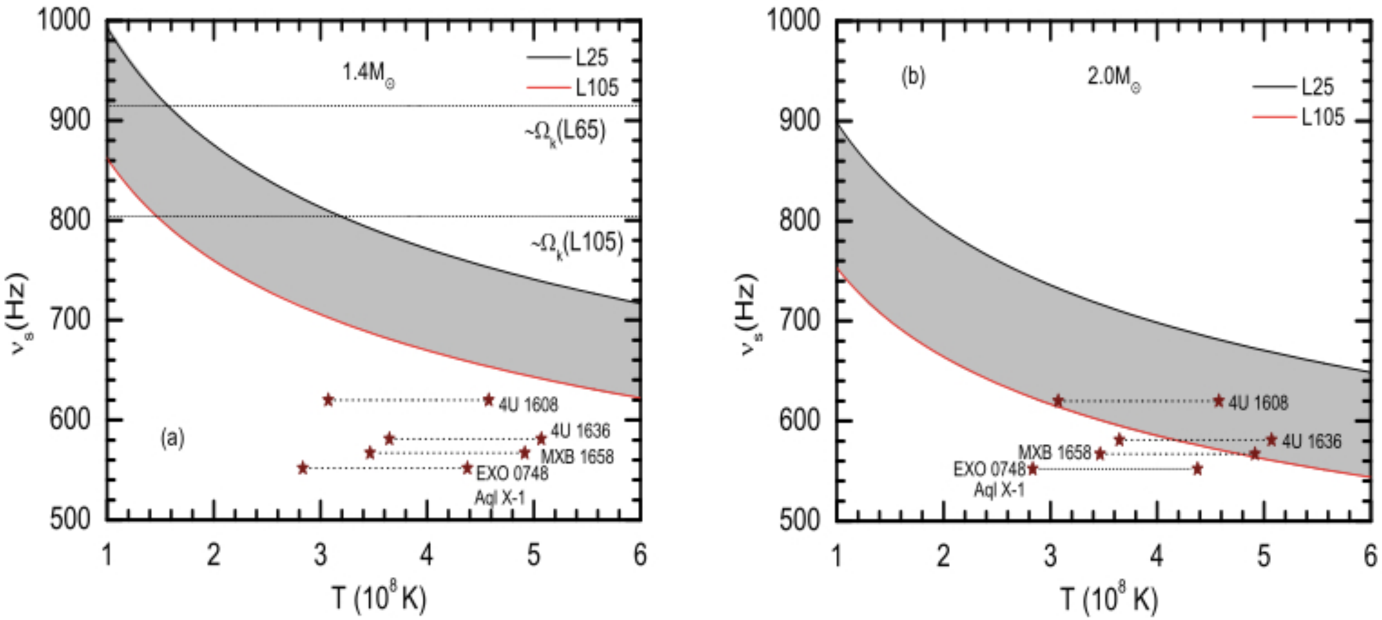

Using electron-electron scattering at the crust-core ($\rho<\rho_0$) boundary as the main dissipation mechanism Wen, Newton & Li obtained L < 60 MeV

Phys. Rev. C 85, 025801 (2012)

The final messages of this talk

- Crust-core transition is sensitive to the symmetry energy: Robust correlation of ρ_t with L. Correlation L-Y_{pt} more disperse due to dispersion on E_{sym}. Correlation of P_t with L difficult to predict. Improvement with combiation of L & K_{sym}

- The r-mode instability region is very sensitive to the symmetry energy: is smaller for models with larger L (increase of with ξ & η L). L dependence of ξ & η can be described by simple power laws $\xi=A_\xi L^{B_\xi}$ & $\eta=A_\eta L^{B_\eta}$

- Constraints from LMXB seems to indicate L < 60 MeV

- You for your time & attention
- The organizers for their invitation
- COST for its support